# Design, simulation and analysis of a *LowTech* Capacitive Micromachined Ultrasonic Transducer (CMUT)

Ismail Jabri*, Etienne Lemaire
*Université de Tours, Polytech Tours, GREMAN, UMR-CNRS7347, F-37200 Tours, France*
*Contact email : ismail.jabri@etu.univ-tours.fr*

A B S T R A C T

This paper introduces a low-tech capacitive micromachined ultrasonic transducer (CMUT) designed with low environmental footprint materials. The fabrication process involves a copper plate as the fixed bottom electrode, a polymer-based adhesive as a dielectric material, and an aluminum foil as the top electrode.
Finite element simulations include studies of displacement, mechanical stresses, and eigenfrequency. Experimental measurements validate the device's electromechanical behavior, showing an eigenfrequency of 88.6 kHz and a displacement of 22 pm. The low-tech CMUT demonstrates potential for applications such as ultrasonic actuation and energy harvesting, offering simplicity, biocompatibility, and low environmental impact. While not directly ready for applications, these transducers provide hands-on experience with technology similar to high-performance silicon-based implementations. These low-tech MUTs are perfect practical case studies for teaching purposes, combining simulation and experimental validation.

*Keywords : Ultrasonic actuation, CMUT, Finite Element Simulation, lowtech, Ecodesign*

## 1. Introduction

In the realm of ultrasonic transducer technology, piezoelectric crystals, ceramics, and polymers materials have long dominated [1]. In recent years, due to the advancement in microfabrication techniques, the capacitive micromachined ultrasonic transducers (CMUT) have emerged as a competitive technology in this field. This technology is based on the principle of combining capacitors with membranes. The basic element of a CMUT cell is a plate capacitor, one of which is fixed, and while the other is a flexible membrane. It operates both in transmission and reception modes [2]. In the transmit mode, by superimposing a DC bias with an AC voltage signal, the membranes oscillate. This oscillation generates acoustical waves, which have a typical ultrasonic frequency. The displacement of the membranes can be of the order of (pm) and can be observed using a laser vibrometer. In the reception mode, incident acoustic waves set the membranes into vibration, modulating the overall capacitance of the device. Under DC voltage, the capacitance variation can be sensed through a readout circuit [3].
CMUTs are often made with materials like silicon, which plays a significant role in the manufacturing process [4]. Nowadays, the demand for this material is rocketing due to its extensive range of use, the ongoing energy transition led by many governments, and also with the proliferation of connected devices. Consequently, the adoption of a low-tech approach [5] [6], prioritizing simplicity, accessibility and lower-energy manufacturing processes, is becoming increasingly crucial for managing the environmental resources of our planet.
This paper introduces the design of a low-tech CMUT followed by a comparison between finite element simulation results and experimental measurements of the displacement and eigenfrequency.

The paper is structured as follows : Section.1 deals with a brief introduction of the CMUT device. Section.2 details the design of the device. Section.3 focuses on finite element simulation. Section.4 covers experimental measurements. The paper concludes with Section.5.

## 2. **Realization of a low-tech CMUT**

Figure 1 illustrates the materials and fabrication steps of the CMUT. A copper plate, covered with a thin insulating layer, serves as the fixed bottom electrode and defines the device's inertia by being a fixed part. Subsequently, a double-sided adhesive layer, 20µm thick and assimilated to polypropylene, is mechanically cut to create square cavities and applied to the copper plate. Next, a 10µm layer of aluminum foil is attached on top of the adhesive to form the top electrode. When considering the materials and manufacturing process employed, the environmental impact of this device is limited [5].

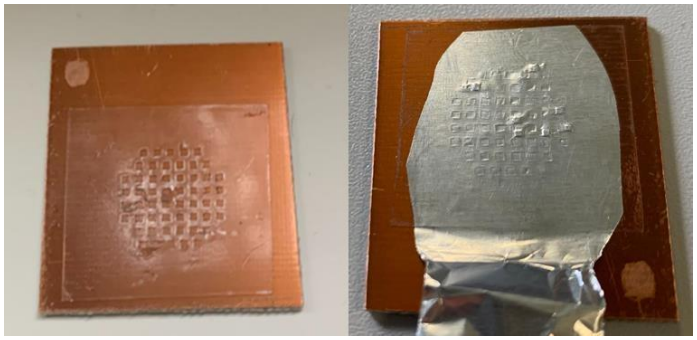

**Figure 1**. Design details of CMUT low-tech.

It is notable that the prototype has larger dimensions compared to industrial CMUTs, resulting in an expected lower frequency behavior.

## 3. **Finite element simulation on COMSOL Multiphysics**

COMSOL Multiphysics is a versatile tool to model the comprehensive functionality of the proposed transducer, including various physics studies [2] [7]. This work focuses on the fundamental analysis of the basic element of a CMUT cell, where Solid Mechanics module of Structural Mechanics Physics study and Electrostatics module of AC/DC Physics study were used to define the boundary conditions. The cell is operating in out-of-plane mode and all edges are kept on fixed constraints as shown in Figure 2. A 235 VDC Bias along with 10 VAC was superimposed on the top membrane. The bottom membrane was kept at ground.
Subsequently, a free tetrahedral mesh of fine size was created for finite element method (FEM) simulations, as shown in Figure 3. Two studies are conducted simultaneously: a stationary study to examine displacement and mechanical stresses, and a second study in the frequency domain to extract the eigenfrequency of the membrane. In addition to the intrinsic constants for each material preloaded by the software, parameters added to the software are outlined in Table 1.

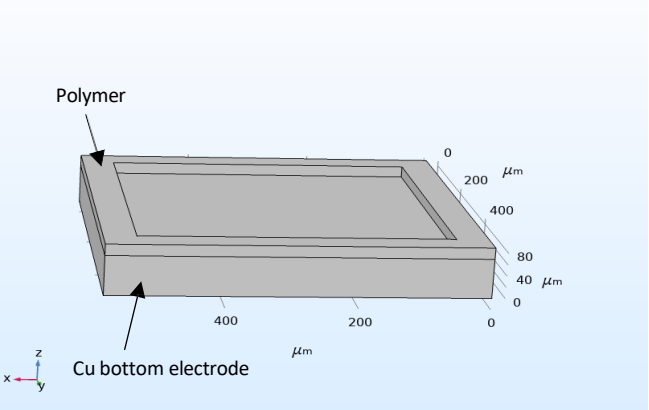


**Figure 2.** Solid model of fixed constraints' cavity.

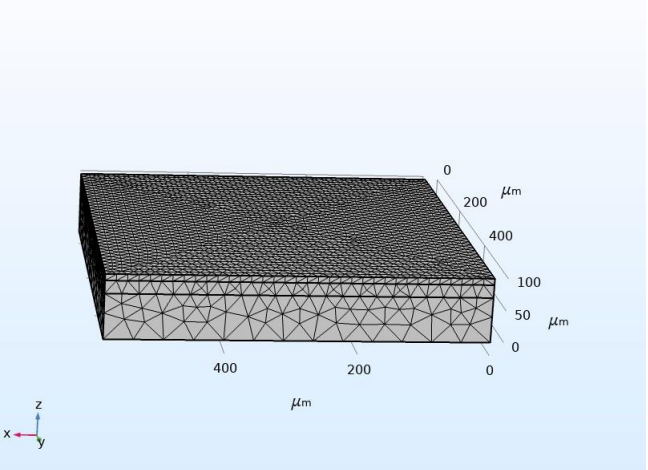


**Figure 3.** Mesh considered for FEM simulation.

**Table 1**

CMUT cell model parameters

| Parameters | Dimensions |
|---|---|
| Bottom electrode thickness | 70 µm |
| Top electrode thickness | 10 µm |
| Side of square cavity | 600 µm |
| Poisson's ratio (for polypropylene) | 0.45 |
| Young modulus (for polypropylene) | 1 GPa |
| Density (for polypropylene) | 930 $kg/m^3$ |

Figure 4. Simulation results: (a) 3D image of "out- of-plane" displacement, (b) membrane deflection as a function of side distance, (c) displacement field arrows when the alternating potential across the CMUT is positive Figure 4 depicts simulation results, offering a comprehensive view of the CMUT's mechanical behavior. The 3D scan showing displacement intensity, provides valuable insights into the distribution of deformation and its maximum zone with a first mode at the eigenfrequency of 80 210 Hz. Figure 4.b deals with the deflection curve along the line through the midpoint of two parallel sides. This representation confirms the results from Figure 4.a by showing a displacement peak of 34 pm, underscoring that the center of the cavity experiences the most significant deflection.
Figure 4.c shows displacement field arrows when the alternating potential across the CMUT is positive. This induces an electrostatic force on the membrane, causing its deformation in that direction.
As for Figure 4.d, it displays the Von Mises stress on a vibrating membrane. This mechanical parameter represents the applied force normalized to the surface area. Examining this measure is crucial for analyzing material resistance to deformations and estimating the likelihood of material failure. In this case, the stress is notably intense at the edges of the cavity compared to the rest of the surface. However, a value of $10^3$ $N/m^2$ remains relatively low compared to the breaking thresholds of aluminum foil, which is $70.10^6 N/m^2$ [8].

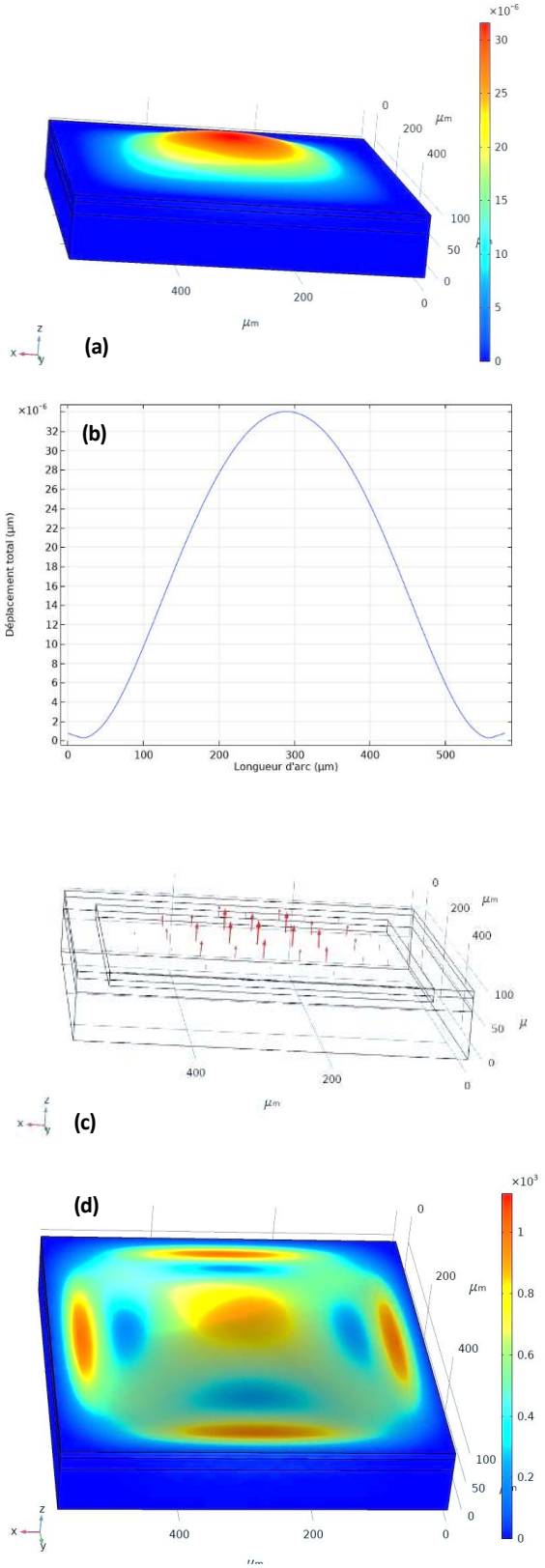


**Figure 4.** Simulation results: (a) 3D image of "out- of-plane" displacement at 80.2 kHz, (b) membrane deflection

as a function of side distance, (c) displacement field arrows when the alternating potential across the CMUT is positive and (d) Von Mises stress on a vibrating membrane

## 4. **Experimental measurements**

### 3.1 Electrical characterization

In addition to the simulation, experimental measurements were conducted to validate the performance of the low-tech CMUT. The first procedure involved supplying the device with DC bias without applying AC voltage, then the overall capacitance is measured for each Vdc using a multimeter, as illustrated in Figure 5.
The initial capacitance value of the CMUT is nearly 230 pF. As the DC bias is incremented, it causes a rise in the electric field $E$ within the structure. This electric field induces an electrostatic force, leading to an attraction of additional charges between the two electrodes. Once the pull-in voltage is passed (not reached in this measurement) the capacitance value is expected to stabilize.

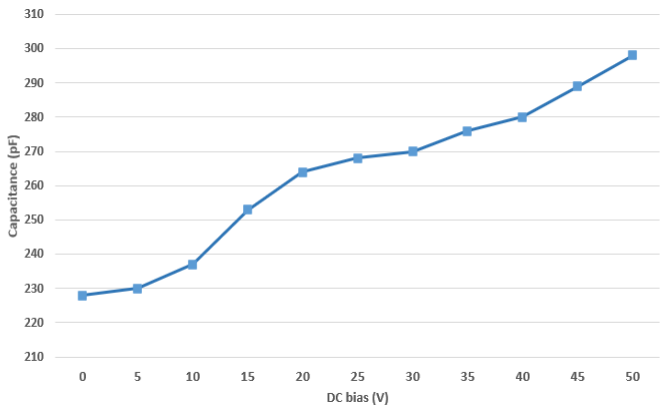


**Figure 5.** Capacitance (pF) as a function of DC bias (V)

### 3.2 Mechanical characterization

The second experiment aims to characterize the mechanical behavior of the CMUT. For this purpose, a laser vibrometer was employed to measure the out-of-plane displacement when the device is subjected to a 10Vpp Chirp signal while varying DC Bias from 0 to 235 V. Audible acoustic waves generated by the CMUT can be perceived from this actuation. After acquiring the displacement curve, MATLAB software was for post-processing operations such as filtering and fitting the data points. Figure 6 presents the results.

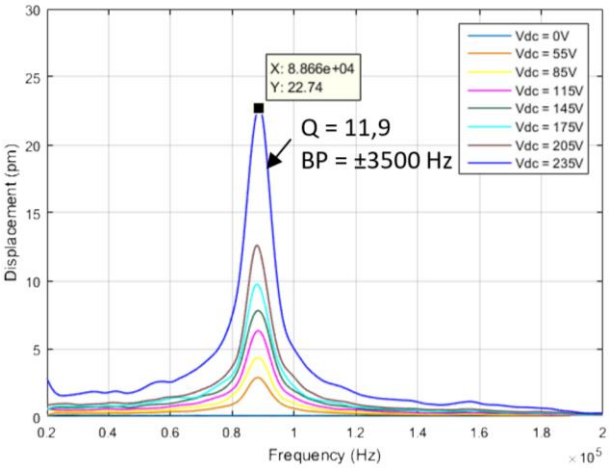


**Figure 6.** Module of displacement (pm) as a function of frequency 0-200 kHz for different DC Bias.

The displacement response of the CMUT is amplified as the DC bias increases . At 235V, dynamic resonance mode had an out-of-plane amplitude exceeding 20 pm. The quality factor Q = 11.9 reflects the ability to operate effectively within a specific frequency range, in this case, ±3500 $Hz$ centered around the central frequency of 88.6 kHz.
The resonance frequency and the maximum displacement obtained in the simulation (80.21 kHz; 34 pm) is in the same order of magnitude as the experimental value (88.6 kHz; 22 pm).
However, the observed disparity could arise from factors like fabrication tolerances, boundary condition differences, environmental conditions influences.

## 5. **Conclusion and perspectives**

In this work, a low-tech CMUT was fabricated and characterized, highlighting a sustainable approach using lower environmental footprint materials and manufacturing processes. The fabrication

involved a copper plate, polymer-based adhesive, and aluminum foil. Comprehensive characterization, involving both simulation and experimental measurements, has been demonstrated. Considering the larger dimensions, the CMUT demonstrated an electromechanical behavior, with an eigenfrequency and displacement exceeding respectively 80 kHz and 20 pm.

These transducers hold potential for various applications including ultrasonic actuation and energy harvesting, thanks to their low material costs compared to any other fabrication techniques. The simplicity, biocompatibility and low environmental impact can unlock the full potential of CMUT low-tech. However, these transducers may not be directly integrated into industrial applications, they serve as excellent candidates for educational purposes, providing hands-on experience with a technology similar to high-performance silicon-based implementations. Thanks to these low-cost MUTs, simulation results could be verified experimentally using tools that can be found in any *fablab*.

## Acknowledgements

Authors would like to thank the Certem: “Centre d'Études et de Recherches Technologiques en Microélectronique” for providing the equipment to measure the electromechanical properties of all micromachined systems.

## References

[1] GOYAL, Rahul et YADAV, Divya Mohan. Design and simulation of a mems-based capacitive micro-machined ultrasonic transducer for viscosity sensing applications. Centre for Nanoscience and Engineering, Indian Institute of Science, 2019.

[2] RAY, Anubhab, CHANDEL, Vivek, TAIWADE, Kajol, et al. Design and analysis of CMUT device using COMSOL for Radio frequency applications. Materials Today: Proceedings, 2022, vol. 65, p. 2602-2605.

[3] ANBALAGAN, S. A., UMA, G., et UMAPATHY, M. Modeling and simulation of capacitive micromachined ultrasonic transducer (CMUT). In : Journal of Physics: Conference Series. IOP Publishing, 2006. p. 595.

[4] X. Liu et al., "A Paper-Based Piezoelectric Accelerometer," 2 Janvier 2018.

[5] E. Lemaire*, "Green paper-based piezoelectrics for sensors and actuators," Sensors and actuators A 244, pp. 285- 291, 2016.

[6] E. Lemaire et al., "Fast fabrication process of low environmental impact," 4 Novembre 2015.

[7] A. Ravi, "Modeling and Simulation of Dual Application Capacitive MEMS Sensor," 2014.

[8] SCHWEITZER S.A.S, "FICHE TECHNIQUE PAPIER ALUMINIUM CUTTER BOX," 04 ,2021.

[9] Hoang-Phuong Phan et al., "GRAPHITE-ON- PAPER BASED TACTILE SENSORS USING PLASTIC LAMINATING TECHNIQUE," Janvier 2015.

[10] G. M. Whitesides et al., "Paper-based piezoresistive MEMS sensors," 2011.

***ECOLE POLYTECHNIQUE DE L'UNIVERSITE DE TOURS***
Electronics and Energy Department,
7, Avenue Marcel Dassault
37200, Tours France
Tel. +33 (0)2 47 36 13 00
polytech.univ-tours.fr

**Additional information**
for the article entitled:
*Design, simulation and analysis of a LowTech Capacitive Micromachined Ultrasonic Transducer (CMUT)*

# Final year project presented by:

**Ismail JABRI**

supported on: **February 22, 2024**

# Design, manufacture and characterization of low-tech microsystems

Project supervised by :

**Mr LEMAIRE Etienne**

---

JURY :

**Mr LEMAIRE Etienne**

**Ms BATUT Nathalie**

# ACKNOWLEDGEMENTS

Before beginning this report, I would like to express my deep gratitude to Mr. LEMAIRE Etienne for his support throughout the project. A special thank you for sharing his know-how during the experiments and for generously giving up his time to bring me back to the CERTEM laboratory to carry out measurements with sophisticated equipment. These experiences have greatly enriched my academic career.

Finally, I'd like to thank Madame Batut Nathalie for organizing the poster/video session, which was a new and formative exercise for me.

# TABLE OF CONTENTS

# TABLE OF FIGURES

# I. Introduction

Microelectromechanical systems (MEMS) stand out as miniaturized components, combining fixed and moving/vibrating elements to achieve electrical transduction [1] [2]. The advent of these microsystems has opened up new perspectives in device miniaturization, giving rise to a diverse range of sensors and actuators, from accelerometers, force or pressure transducers to medical imaging...

These microsystems are often based on semiconductor materials such as silicon, which plays a major part in the manufacturing process [3].
Today, demand for these materials continues to grow due to their broad spectrum of uses, especially with the energy transition and the increasing adoption of electrical technologies, as well as with the expansion of the Internet of Things (IoT) [4] and the proliferation of connected devices. Consequently, adopting a low-tech approach, favoring simplicity, accessibility and less energy-intensive manufacturing processes [4] [5], is becoming increasingly crucial to managing our planet's environmental resources.

In this context, this project aims to design, manufacture and characterize three types of low-tech microsystems for educational use. The first type is the CMUT (Capacitive Micromachined Ultrasonic Transducer), using flexible membranes to generate ultrasonic waves. The second type focuses on cantilevers, which are MEMS cantilever beams. The third is an electromagnetic transducer in the form of a U-shaped wire.

This document adopts the following structure: Section 1 provides a brief introduction to the project background and defines the objectives. Next, each transducer type is dealt with in a dedicated chapter, covering design and characterization in detail. Finally, the document concludes with a general summary of the project, followed by perspectives for future developments.

## II. CMUT (Capacitive Micromachined Ultrasonic Transducer)

### 1. Operating principle

CMUTs (Capacitive Micromachined Ultrasonic Transducers) are ultrasonic transducers that exploit the principle of variable electrical capacitance to convert the mechanical energy of an ultrasonic wave into an electrical signal, and vice versa. This technology is based on the principle of combining capacitors and membranes [6] [7]. The basic element of a CMUT cell is likened to a planar capacitor, with one electrode fixed and the other a flexible membrane. The system operates in both transmit and receive modes, as shown in Figure 1.

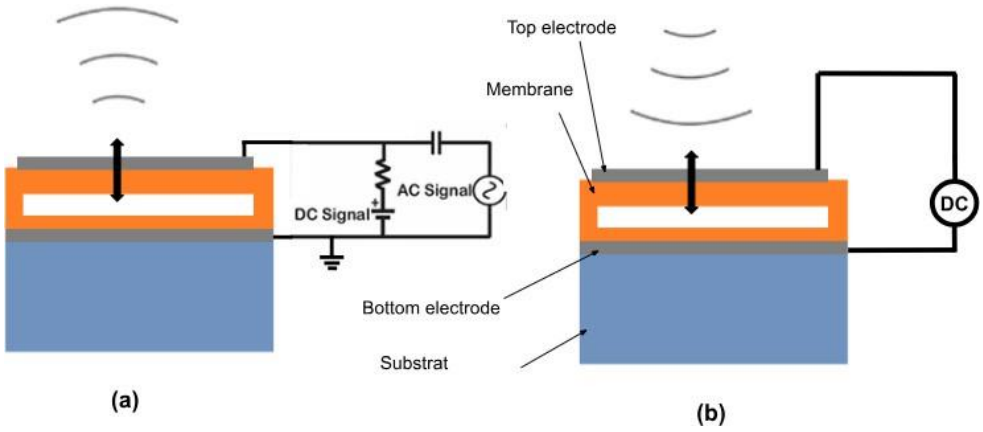


***Figure 1:*** *Principle of the CMUT (a) in transmission powered by DC superimposed on an AC voltage to generate an ultrasonic wave, and (b) in reception powered only by DC voltage to polarize it.*

In transmission mode, when a DC voltage is superimposed on an AC voltage, the diaphragms oscillate. This oscillation generates acoustic waves with a typical ultrasonic frequency. The displacement of the membranes can be of the order of (pm) and can be observed using a laser vibrometer. In receive mode, the incident acoustic waves set the membranes into vibration, modulating the CMUT's overall capacitance, which is supplied with DC voltage. This variation can be detected via an output readout circuit.

### 2. Design and materials

After extensive bibliographical research into the CMUT's operating principle and possible geometries. The first step was to design the device, including the cavity geometry. The Silhouette Studio tool was used for all mechanical cutting operations. In this way, we were able to

Inkscape was used to draw finer structures for laser cutting.

As explained earlier in this document, the aim is to manufacture all the devices using materials that are accessible, less expensive and have the lowest possible environmental impact.

A copper plate, commonly used for printing printed circuits, covered with a thin layer of insulator, serves as the bottom electrode and defines the device's inertia by being a fixed part. Next, a double-sided adhesive layer, 25 µm thick, is cut to create square cavities and applied to the copper plate. Finally, a 10 µm layer of aluminum foil is attached to the adhesive to form the top electrode. Figure 2 shows some examples of this process:

***Figure 2:*** *Low-Tech CMUT manufacturing details*

For a CMUT with a surface area of 3 cm². The initial capacitance measured on the multimeter is $C_0 = 233$ pF. The nature of the polymer can be identified using the relationship of a plane capacitor:

$$C_0 = \frac{\varepsilon_0 \varepsilon_r S}{e}$$

With $\varepsilon_0 \varepsilon_r$ the permittivity, *S* is the surface area of the sample and $e$ is the thickness between the two electrodes.

$$\varepsilon_r = \frac{C_0 e}{\varepsilon_0 S} \quad => \quad \varepsilon_r = \frac{233\times10^{-12}\times25\times10^{-6}}{8.854\times10^{-12}\times3\times10^{-4}} = 2.192$$

The polymer with the closest dielectric constant to this value, while still frequently used industrially for adhesive applications, is polypropylene. Its dielectric constant lies between 2.2 and 2.3. This material is therefore used as a dielectric.

## 3. Finite element simulation

COMSOL Multiphysics is a numerical simulation software package based on the finite element method. It has the particularity of coupling physical phenomena for simulation. The operation of the proposed transducer can be fully modeled with this tool. In this work, the simulation focuses on the fundamental analysis of a CMUT cell [7] [1]. For this, the modules used are solid mechanics (belonging to the physical study of structural mechanics) and electrostatics (belonging to the AC/DC physical study). For the boundary conditions, an embedding (fixed constraints) is imposed on the lower electrode and all edges, as shown in figure 3.a. A polarization of 235 Vdc and 10 Vac has been superimposed on the upper membrane. The potential of the lower membrane is maintained at ground.
Next, a fine tetrahedral mesh was created to perform the finite element method (FEM) simulation, as shown in figure 3.b.

Two studies are carried out simultaneously: a stationary study to examine diaphragm displacement and mechanical stress, and a second study in the frequency domain to extract the diaphragm's natural frequency of vibration.
Since polypropylene does not exist in COMSOL, it has been replaced by polyethylene, which has a dielectric constant close to that of COMSOL. It has been replaced by polyethylene, which has a dielectric constant close to 2.3. In addition to the intrinsic constants for each material previously loaded by the software, the simulation parameters added to the model are presented in Table 1.

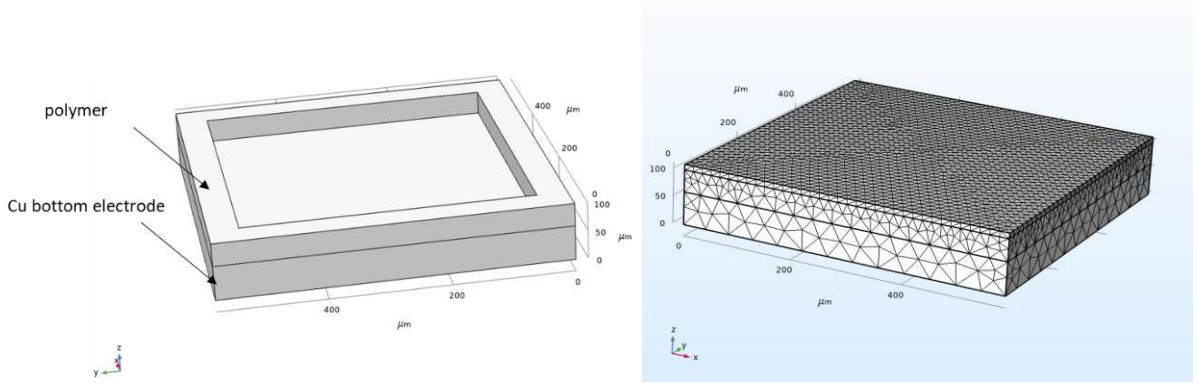


(a) (b)

***Figure 3:*** *(a) Solid model of fixed stress elements and (b) Fine tetrahedral mesh for finite element simulation.*

***Table 1:*** *CMUT cell simulation parameters*

| Parameter | *Value* |
|---|---|
| Lower electrode thickness | $70\ \mu m$ |
| Upper electrode thickness | $10\ \mu m$ |
| Side of a square cavity | $600\ \mu m$ |

| | |
|---|---|
| Poisson's ratio (of polyethylene) | *0.45* |
| Young's modulus (of polyethylene) | *1^E 9 Pa* |
| Density (of polyethylene) | *930 kg/m 3* |

Figure 4 shows the simulation results, providing a comprehensive view of the CMUT's mechanical behavior. Figure 4.a shows the out-of-plane displacement intensity. It provides information on the deformation distribution and its maximum zone. Note that the diaphragm's natural mode is at frequency 80.210 kHz.

Figure 4.b shows the deflection curve along the line passing through the middle of two parallel sides. This representation confirms the results of Figure 4.a, showing a displacement peak of 34 pm, underlining that the center of the cavity undergoes the greatest deflection. Figure 4.c shows the arrows in the displacement field when the alternating potential across the CMUT is positive. This induces an electrostatic force on the membrane, causing it to deform in this direction.

Figure 4.d shows the Von Mises stress on a vibrating cell. This mechanical quantity represents the force applied to a unit area. It is important to examine this quantity to analyze the resistance of materials to deformation and estimate the probability of material failure. In this case, the stress is particularly intense at the cavity stops compared to the rest of the surface. Nevertheless, $10^3$ N/m$^2$ is still a relatively low value compared to the breakage thresholds of aluminum foil, which is $70$ N/mm² = $70 \times 10^6$ N/m².

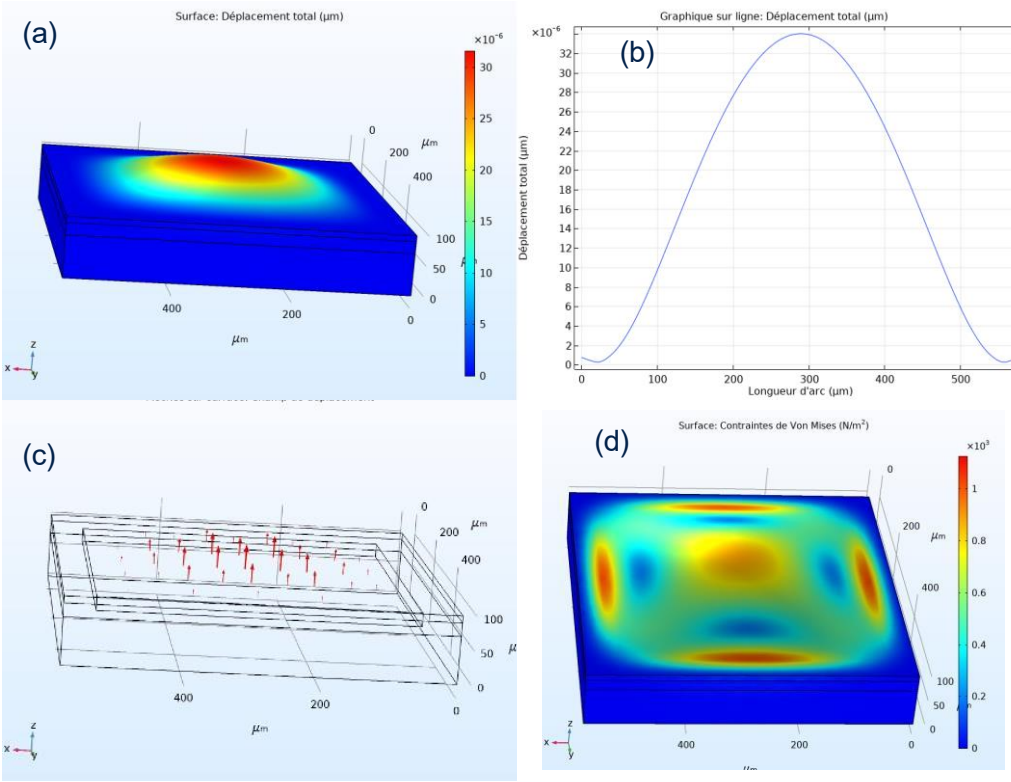


***Figure 4**: Simulation results: (a) 3D image of cavity displacement, (b) membrane deflection as a function of lateral distance, (c) arrows of*

*displacement field when the alternating potential across the CMUT is positive and (d) Von Mises stresses on the vibrating cell.*

Finite element simulation provides an in-depth understanding of CMUT behavior. It provides an idea of how the system works, estimates empirical quantities and optimizes its design before the manufacturing phase. However, this simulation has certain limitations: accuracy depends largely on the fineness of the mesh. In addition, it does not take into account the state of the material over time, such as wear and tear, or environmental conditions.

## 4. Measurement and characterization

### *a. Capacitive behavior*

In addition to simulation, experimental measurements were carried out to validate the performance of the low-tech CMUT. The first step was to supply the device with a DC voltage without applying an AC voltage, then measure the overall capacitance for each Vdc using a multimeter, as shown in Figure 5.

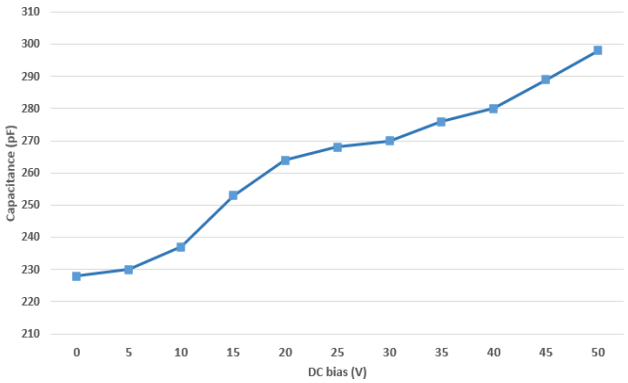


***Figure 5:*** *Capacitance in pF vs. DC voltage in V.*

The initial capacitance value is close to 230 pF. As the DC voltage increases, the electric field E within the structure increases. This electric field induces an electrostatic force, leading to the attraction of additional charges between the two electrodes.

Once the collapse voltage is exceeded, not reached in this measurement, the equivalent capacitance value should stabilize [8].

In a second step, the DC voltage is maintained at 20 V, and a 10 Vpp square-wave signal with a frequency of 3500 Hz is injected into the AC input.

The response of the CMUT, recorded with the oscilloscope, is shown in figure 6. The blue curve represents the input signal, while the yellow curve represents the output signal. We can clearly see that capacitive behavior is very present throughout the exponential charge and discharge. However, when the membranes vibrate, an acoustic wave is generated. It was expected that the output signal would be distorted, containing one or more echoes. Due to the very low amplitude of the membrane displacement shown in figure 4.a, visualizing the desired signal with the oscilloscope at hand becomes arduous. In order to obtain more precise characteristics, it becomes necessary to carry out measurements with more sophisticated equipment.

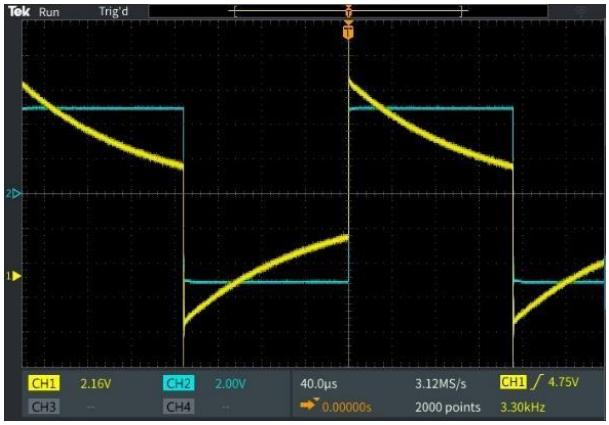


***Figure 6:*** *Time response of the CMUT excited by a square-wave signal*

### *b. Vibratory behavior*

#### *i. Laser vibrometer measurements*

A laser vibrometer is a non-contact vibration measurement sensor. It consists of a monochromatic light source (laser) and an interferometer for measuring the Doppler effect due to the vibration between the emitted and reflected signals [9]. From this interferometry between the 2 signals, the displacement, frequency and phase of the vibration can be deduced...

A pseudo-periodic signal (Chirp) of amplitude 10 Vpp is superimposed on a DC component varying between 0 and 235 V. Next, diaphragm displacement is measured as a function of frequency between 0 and 200 kHz, as shown in Figure 7.

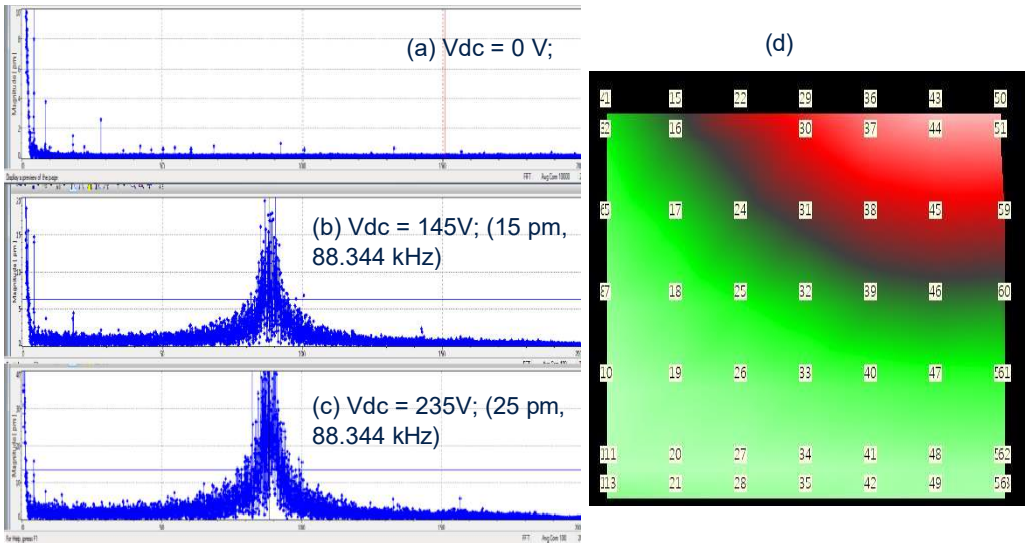


***Figure 7:*** *Displacement in pm as a function of frequency at : (a) Vdc =0V, (b) Vdc = 145 V and (c) Vdc = 235 V. (d) 3D scan of the cavity at Vdc = 235 V*

In the absence of a DC component, the diaphragms do not vibrate. However, as the DC voltage increases, the amplitude of the out-of-plane displacement gradually increases. At Vdc = 145 V, this amplitude reaches around 15 pm, then at 235 V it rises to around 25 pm. The DC voltage is high because of the CMUT's larger dimensions. In this case, more electrostatic force is needed to actuate the membranes. This results in a higher bias voltage.

The measured frequency of the diaphragm vibrations is 88.344 kHz. These results are of the same order of magnitude as the values obtained by simulation (80.21 kHz; 34 pm). Nevertheless, the disparity observed could be due to factors such as manufacturing tolerances, differences in boundary conditions, influences of ambient conditions...

Figure 7.d shows where the displacement is most intense (in red), while less-impacted areas are shown in green. However, during scanning, the laser beam was not focused on the center of the cavity.

### *ii. Post-processing with Matlab*

After acquiring the laser vibrometer measurements, the Matlab tool is used for post-processing operations such as filtering, interpolation...

To extract the bandwidth and quality factor, the data from the displacement vs. frequency curve at 235V (see figure 7.c) are averaged, then filtered using a second-order Butterworth filter. Figure 8.a shows the resulting curve. To improve the representation of the 3D scan of the cavity shown in figure 7.d, a new visualization was generated using Matlab (see figure 8.b).

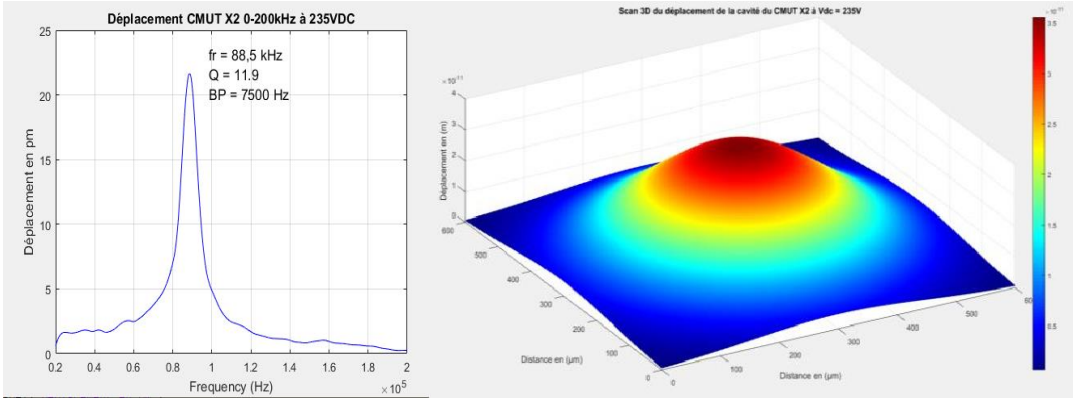


(a) (b)

***Figure 8:*** *(a) Filtered displacement at Vdc = 235 V and (b) 3D scan of the membrane as a function of cavity dimensions.*

The quality factor Q = 11.9 reflects the CMUT's ability to operate efficiently in a specific frequency range, which in this case is +/-3500 Hz centered around the 88.5 kHz center frequency. The transducer can therefore be operated around this frequency.

An equally important characteristic to consider is the actuation force applied to a diaphragm following actuation.

Knowing that the density of aluminum is $2700\ \mathrm{kg/m^3}$. The volume of a square cavity with a side length of 600 µm and a thickness of 10 µm is $3.6 \times 10^{-12}\ \mathrm{m^3}$. Consequently, the equivalent mass of a membrane is estimated to be approximately $1 \times 10^{-2}\ \mathrm{mg}$.

Considering that the mechanical forces applied to the diaphragm are weight and actuation force (see figure 9). The fundamental principle of dynamics can be applied:

$$\sum \vec{F}_{ext} = \vec{P} + \overrightarrow{F_{act}} = m\vec{a}$$

$$P \pm F_{act} = m.a$$

With $P = m.g$

$F_{act}$: the membrane's actuating force.

$m$: the mass of a membrane.

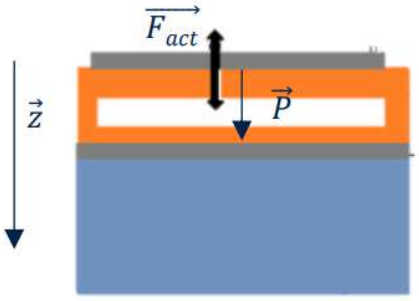


***Figure 9****: Forces applied to the membrane*

$a = (2\pi f)^2 * displacement$: the vibration acceleration [10].

Figure 10 shows the actuating force applied to a diaphragm, both when it is in the same direction as the weight, and when it is in the opposite direction.

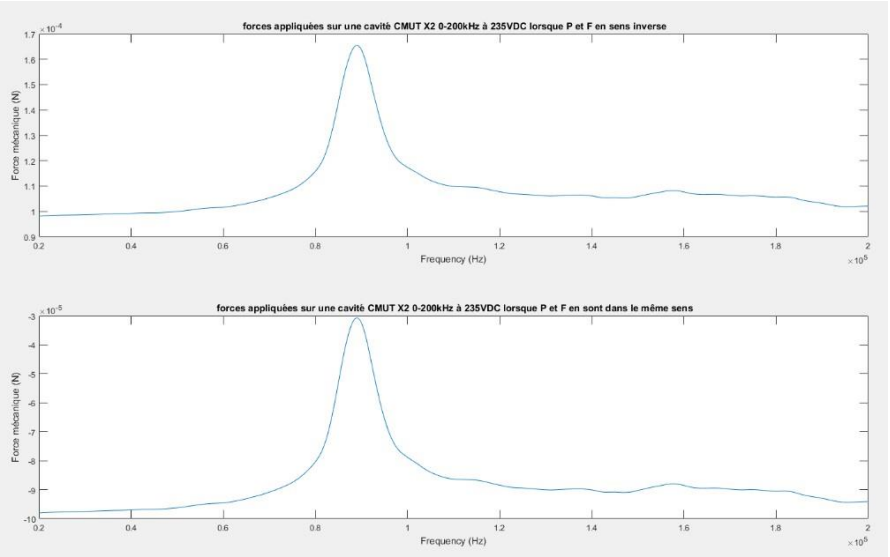


***Figure 10:*** *Case study of the modulus of the actuating force applied to the membrane*

The maximum actuating force applied to a diaphragm is of the order of $1.7 \times 10^{-4}$ □. It is directly related to the motion of the cavity. It can be important to monitor this force on the cavity for common reasons such as: detecting unexpected or excessive variations that can lead to mechanical failure. And therefore to get an idea of the system's durability. In this case, the force applied to a diaphragm remains acceptable given the dimensions of the cavity.

Once the vibration force has been calculated, the mechanical impedance of the system, expressed in N.s/m, can be evaluated using the following relationship:

$$Zm = \frac{F_{act}}{v}$$ Where the vibration velocity $v = 2\pi * f * displacement$ [10].

Figure 11 shows the response obtained in logarithmic scale: $20 \times \log_{10}(Z_m)$.

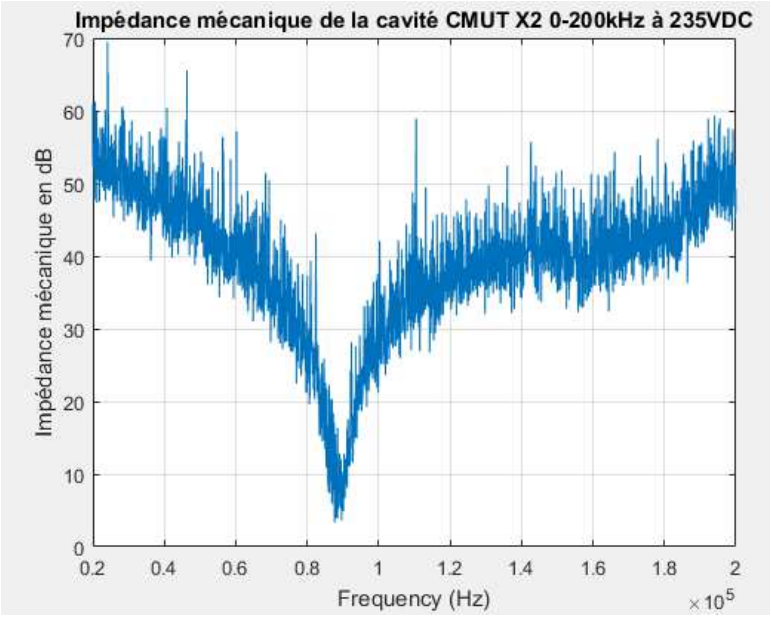


***Figure 11:*** *Mechanical impedance dB as a function of frequency.*

Mechanical impedance is a measure of the resistance to movement of a structure subjected to a given periodic force [11]. From this curve, we can see that mechanical impedance reaches a minimum at the frequency of the membrane's natural mode. This means that the latter is less resistant to the actuating force, leading to an amplified response at this specific frequency.

Finally, sensitivity, in pm/Vdc, is a measure of the device's response to a change in DC voltage. It is defined as the ratio between maximum displacement (expressed in picometers) and applied DC voltage (expressed in volts).

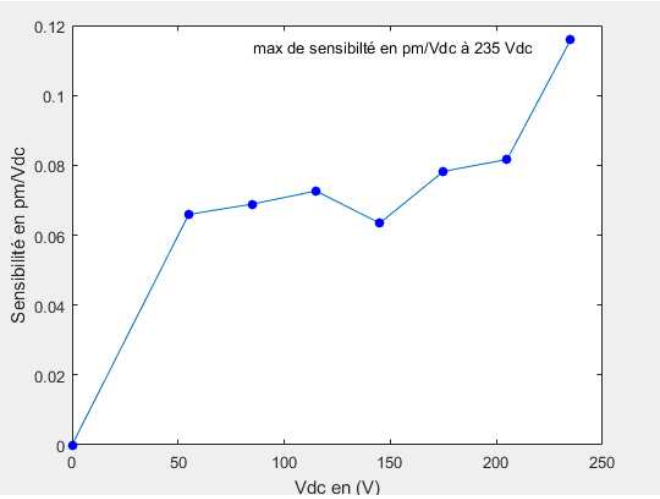


***Figure 12:*** *CMUT sensitivity in pm/Vdc*

This measurement quantifies the CMUT's ability to amplify displacement in response to a DC voltage change. It has a limitation, given the limited number of data points available.

# III. Cantilevers

## 1. Operating principle

Cantilevers also stand out as vibrating structures that find applications as force, density and gas sensors, or in biology (e.g. weighing antigen/antibody interactions). These devices are highly capable of deforming in response to external forces. Cantilevers are often actuated by sticking them on top of a piezoelectric material. When a voltage is applied to the piezoelectric material, the latter deforms in response to this voltage, causing the cantilever to flex.

## 2. Design and materials

Still following the low-tech approach, the cantilevers are made of copper or metallized PET films cut using mechanical die-cutting. The piezoelectric material used for actuation is Rochelle salt. This material is a crystal with highly temperature-dependent piezoelectric properties, existing up to a maximum of 45°C [12] [13]. Figure 13 shows details of the design and materials used.

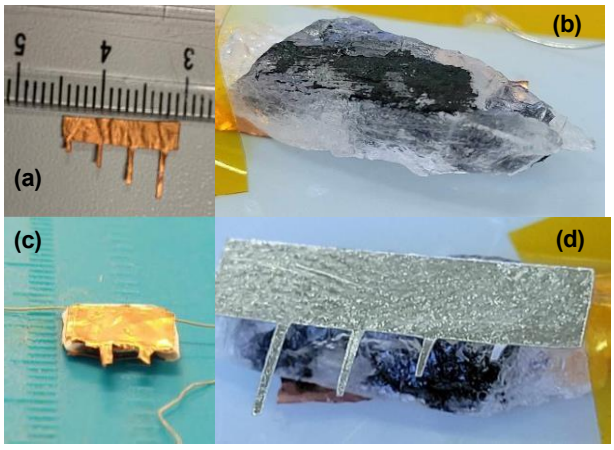


***Figure 13:*** *(a) beams of different sizes, (b) La Rochelle salt, (c) and (d) piezoelectric salt-actuated beams*

Impedance analysis was carried out on La Rochelle salt using an impedance meter. Its electrical properties are shown in figure 14.

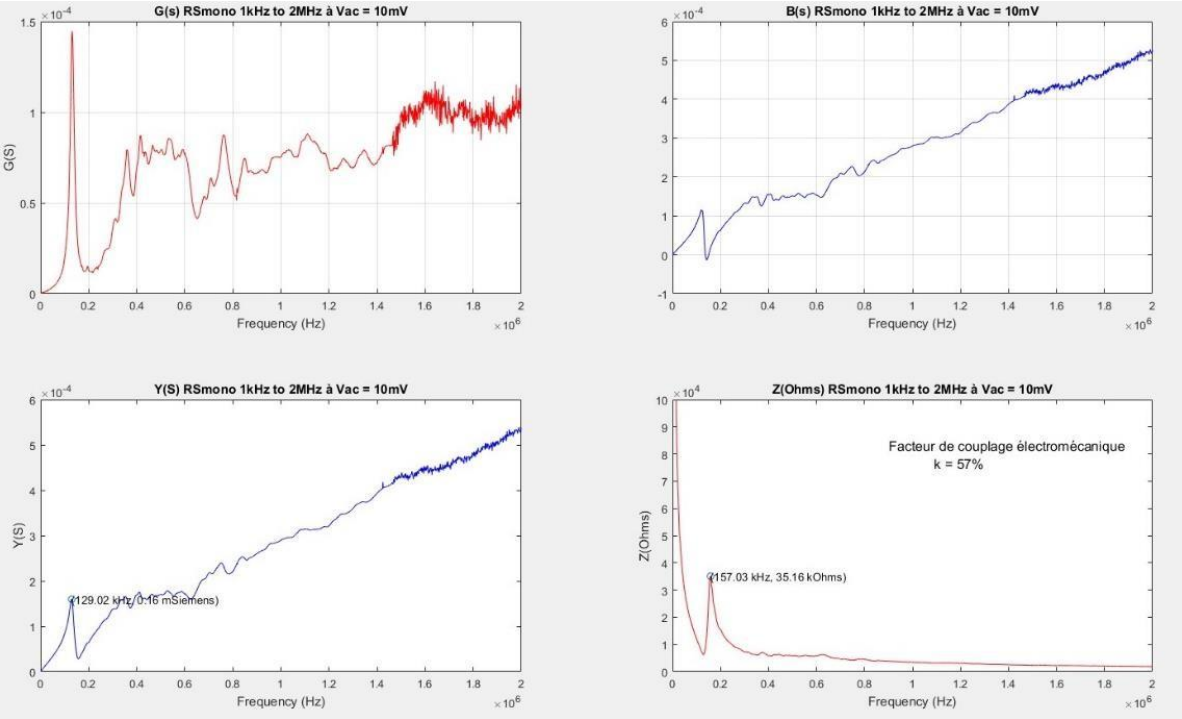


***Figure 14:*** *Conductance G(s), susceptance B(S), admittance Y(S) and impedance Z(Ohms) of La Rochelle salt as a function of frequency 1 kHz - 2 MHz.*

The G(S) conductance curve visualizes the different modes of the piezoelectric salt, including a predominant mode near 200 kHz.

On the other hand, by examining the impedance curve Z(Ohms), we can deduce the anti-resonance frequency, corresponding to the point where impedance reaches its maximum, and this frequency is set at 157.03 kHz. In parallel, the Y(S) admittance curve allows us to deduce the resonance frequency, identified as the maximum admittance point, and this frequency is measured at 129.02 kHz. These two quantities, the anti-resonance frequency and the resonance frequency, are used to calculate the salt's electromechanical coupling factor, which reflects the efficiency with which the material can convert electrical energy into mechanical energy and vice versa.

Its formula is as follows [14] :

$$k = \sqrt{\frac{(f_{ar}^2 - f_r^2)}{f_{ar}^2}} = 57\%$$

## 3. Finite element simulations

As in the CMUT section, simulation of this type of transducer is important in order to understand their vibratory behavior, estimate the frequency of the beam eigenmodes and displacement amplitude. The structural model simulated is as follows:

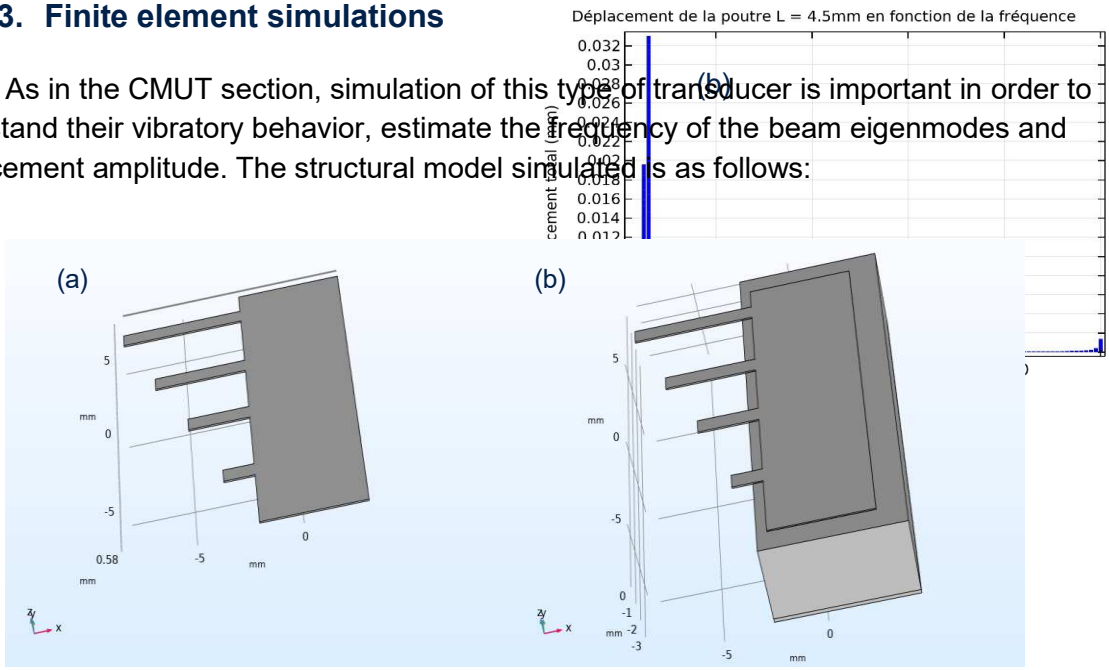


***Figure 15:*** *(a) Model of beams of different sizes and (b) complete structural model simulated on COMSOL*

The material used to simulate the beams is copper. The study is similar to that carried out on the CMUT, in terms of the modules used (solid mechanics and electrostatics). For the boundary conditions, a fixed stress is imposed on the lower electrode and on all edges, as shown in figure 15.b. Two studies are carried out simultaneously: a stationary study to examine the displacement of the beams, and a second study in the frequency domain to extract their natural frequencies.

The simulation provides results for all the beams. However, for the purposes of this study, only the beam of length L = 4.5 mm will be treated for comparison with experimental measurements.
The results are shown in Figure 16.

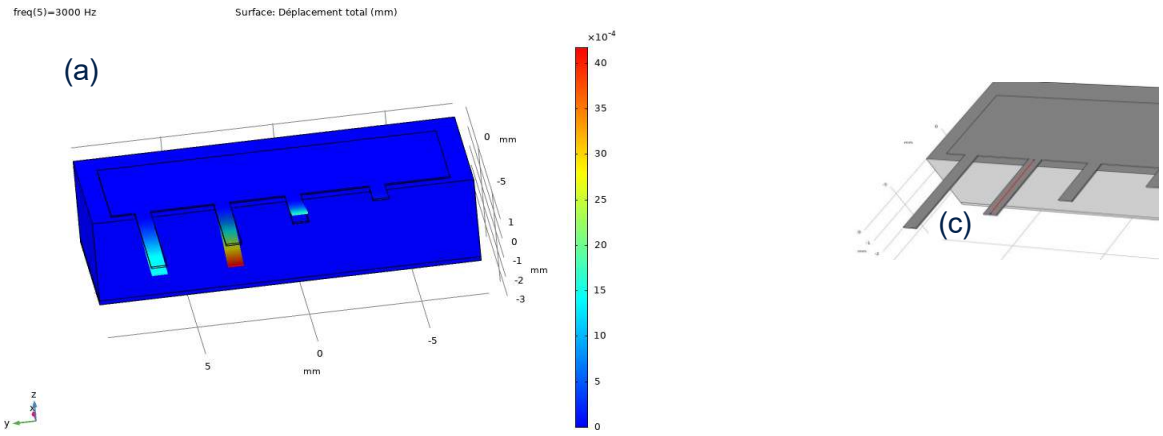


***Figure 16:*** *(a) Beam displacement amplitudes at 3000 Hz, (b) displacement amplitude as a function of frequency along (c) the cut line of the beam length L = 4.5 mm*

Figure 16.a shows the amplitude of the beam displacement at the 3000 Hz frequency, which is of the order of 400 picometers (pm). Figure 16.b shows a histogram of the displacement contributions for each frequency, for each point of the cut line shown in figure 16.c. The next step is to compare these results with experimental measurements.

## 4. Measurement and characterization

In addition to simulation, experimental measurements were carried out to validate the transducer's performance. The system studied is that shown in figure 10.d.

The Rochelle salt is actuated by a pseudo-periodic signal (Chirp) of amplitude 10 Vpp. Next, the displacement of the beam of length L = 4.5 mm is measured as a function of frequency between 0 and 100 kHz, using the laser vibrometer, as shown in figure 17.

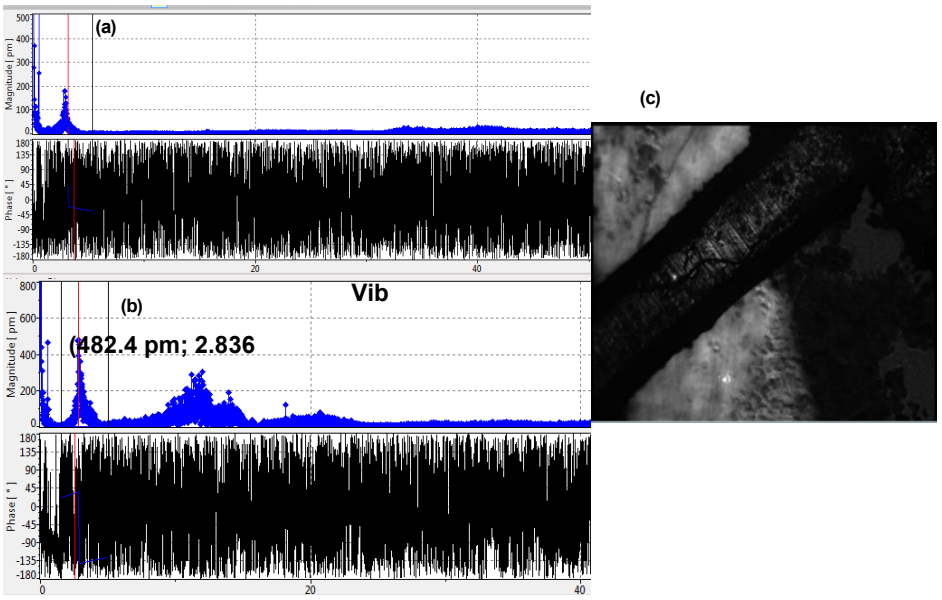


***Figure 17:*** *(a) Eigenmode of beam only, (b) eigenmodes of beam and Rochelle salt and (c) beam viewed with vibrometer.*

The beam exhibits a principal eigenmode at 2836 Hz with a displacement amplitude of 482 pm. This result is in line with that obtained from the simulation in figure 16.a, while the other observed modes are related to the Rochelle salt piezoelectric crystal. A particular resonance is that at which the beam vibrates most intensely. This resonance induces a phase discontinuity, marked by a 180° change. However, due to noise in the phase diagram, this feature is not visualized.

These vibration modes are of significant importance in a variety of applications. They are useful for detecting undesirable vibrations (e.g. pressure variations in the ambient environment). They are also used to detect the density of gases.

It should be noted that the electromechanical coupling between the beams and the

piezoelectric salt is not optimized due to the roughness of the salt surface, and poor adhesion of the beams to the salt.

## IV. Electromagnetic transducer: U-shaped wire

### 1. Operating principle

The final type of transducer discussed in this document is the U-wire electromagnetic transducer, which is a non-contact type of actuation. This type of transducer is based on the principle of Lorentz force, also known as magnetomotive force. This principle is based on the interaction between an electric current flowing through a conductor and a magnetic field.

In this case, a thin copper wire is placed in a magnetic field, generating a force that induces mechanical displacement. This principle is used in a variety of applications, such as electrodynamic microphones, whose sound waves cause vibrations in a diaphragm, generating an electrical signal.

This type of transducer is versatile. It can be powered by alternating voltage (AC) to induce oscillations in the U-wire, enabling detection of unwanted vibrations such as pressure variations. Alternatively, it can be supplied with direct voltage (DC), in which case variations in the orientation of the U-wire will be captured, extending its detection capability.

Figure 18 shows a schematic diagram of this electromagnetic transducer.

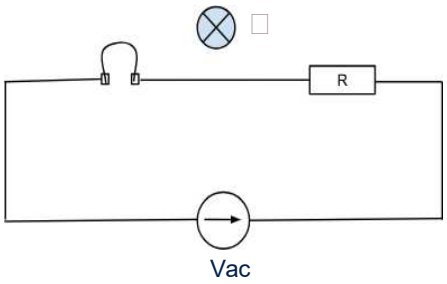


***Figure 18**: Diagram of the electromagnetic transducer*

The resistor is 10 ohms. It limits the current and prevents short-circuiting. The positioning of the U-shaped wire in the magnetic field is shown in figure 19.

***Figure 19**: U-shaped copper wire between two magnets*

Silicone paste is used to fix the magnet support. It's important to note that the magnets must be as close as possible to the wire, without the wire coming into contact with the magnets.

## 1. Measurement and characterization

We are now interested in the equivalent electrical impedance of the system. The impedance meter is calibrated at short-circuit. The curves shown in figure 20 are visualized.

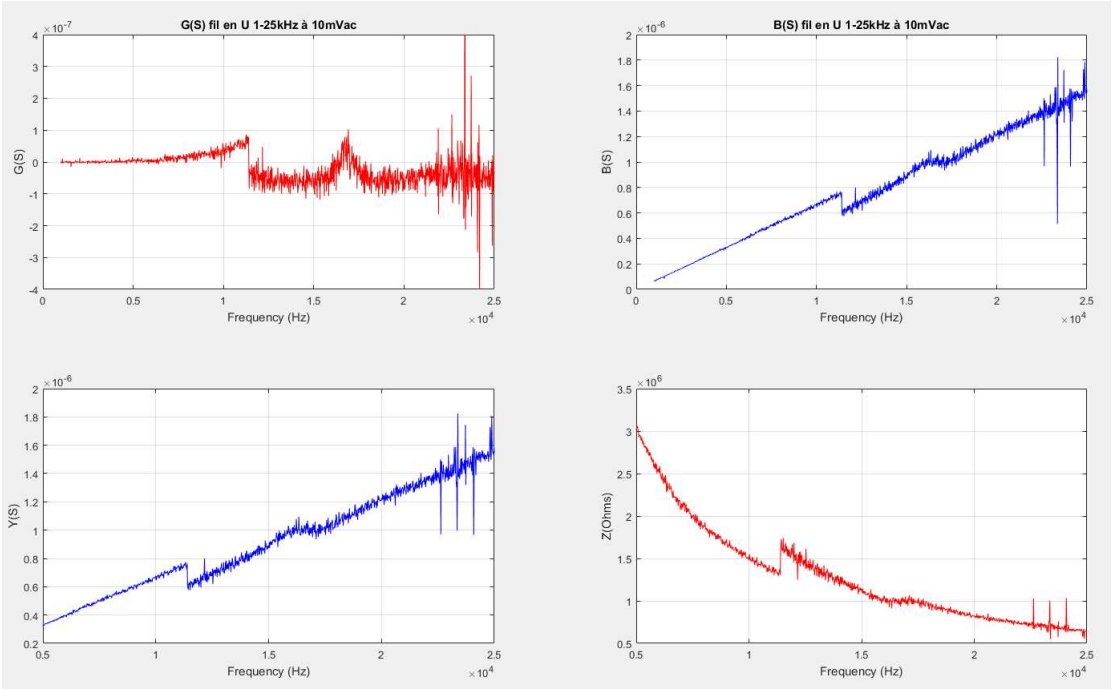


***Figure 20:** Conductance G(s), susceptance B(S), admittance Y(S) and impedance Z(Ohms) of U-wire salt as a function of frequency 5 kHz - 25 kHz*

When impedance measurements do not provide a clear picture of electrical behavior

(e.g. resonance) due to small variations or the dominance of the reactive part, it can be useful to look at the conductance G(S) to obtain more information.

On the G(S) conductance figure, two patterns can be seen. The first is a display jump provided during acquisition of this curve. The second is the resonance of the U-wire around the 16 kHz frequency. This transducer can be used around this frequency range in loudspeakers, in particular for selective amplification. In other words, amplify only frequencies close to 16 kHz.

Note that system response depends on several factors, particularly wire length, cross-section and surrounding magnetic field. To maximize response amplification, it's essential to orient the magnetic field lines perpendicular to the wire's cross-sectional area. This arrangement favors the induction phenomenon, generating more induced current.

In addition, to minimize losses in the magnetic field lines, it would be wise to channel them through a metal part rather than leaving them in the air.

# V. Conclusion and outlook

In conclusion, this project focused on the design, manufacture and characterization of three types of low-tech microsystems for educational purposes: the CMUT (Capacitive Micromachined Ultrasonic Transducer), cantilevers and the U-wire electromagnetic transducer.

The materials used in the design are accessible, less expensive and with less ecological impact, such as: copper, aluminum foil or metallized PET for the metals, polypropylene as dielectric material and La Rochelle salt as piezoelectric material. Finite element simulation was used to understand the physical behavior of these transducers, with particular emphasis on membrane displacement, mechanical stress and natural frequencies. Characterization of these microsystems, based on experimental measurements, validated their performance.

CMUTs, with a composite dielectric between polypropylene and air, remain less resonant systems. Miniaturization results in a higher resonant frequency, improving the spatial resolution of non-destructive detection. Future prospects offer the possibility of using a dielectric material with a higher constant and employing a low-noise amplifier (LNA) to further exploit the electrical transduction of CMUTs [15]. As for cantilevers, detection accuracy increases when the vibration behavior (eigenmodes) is well defined. In other words, the successive eigenmodes are far enough apart. For the U-wire electromagnetic transducer, the operating principle based on the Lorentz force was explained, and electrical impedance measurements provided crucial information on the frequency range exploitable for these transducers and the factors influencing its performance.

The adopted low-tech approach focused on simple manufacturing processes with low energy consumption. The results obtained, whether from simulations or experiments, have demonstrated that these microsystems are good candidates for experimenting with behavior similar to high-performance industrial microsystems [4] [5].

On a personal level, this project was an opportunity to deepen my knowledge of sensor physics, reinforce my MATLAB skills and self-train on COMSOL. Last but not least, this experience not only enriched my technical skills, but also familiarized me with the importance of the low-tech approach.

## VI. References


[1] A. Ravi**, "Modeling and Simulation of Dual Application Capacitive MEMS Sensor," 2014.

[2] W.Yu Liu et al., "Paper-based piezoresistive MEMS sensors". 2018

[3] Yu-Hsuan Wang et al., "A Paper-Based Piezoelectric Accelerometer," January 2, 2018.

[4] E. Lemaire et al., "Green paper-based piezoelectrics for sensors and actuators," *Sensors and actuators A 244,* pp. 285-291, 2016.

[5] E. Lemaire, "Fast fabrication process of low environmental impact," November 4, 2015.

[6] A. Boulmé, "DESIGN AND CHARACTERIZATION OF CMUT WIDE-BAND PROBES FOR CONVENTIONAL IMAGING AND ASSESSMENT OF BONE TISSUE," 2013.

[7] H. Anubhab Ray et al., "Design and analysis of CMUT device using COMSOL for Radio frequency," *Proceeding 65,* pp. 2602-2605, 2022.

[8] Yongli Huang et al., "Comparison of Conventional and Collapsed Region Operation of Capacitive Micromachined Ultrasonic Transducers," October 10, 2006.

[9] Wikipedia, "Vibrometer laser," [Online online]. Available: https://fr.wikipedia.org/wiki/Vibrom%C3%A8tre_laser.

[10] M. J. Griffin, "Encyclopedia of Occupational Safety and Health," [Online]. Available: https://www.ilocis.org/fr/documents/ilo050.htm.

[11] Wikipedia, "Impedance mechanical," [Online online]. Available: https://fr.wikipedia.org/wiki/Imp%C3%A9dance_m%C3%A9canique.

[12] E. Lemaire et al., "Note de synthèse pour bien démarrer avec la réalisation de transducteurs piézoélectriques en Sel de Rochelle (avec électrodes)," November 17, 2020.

[13] Wikipedia, "Salt from seignette," 2023. [Onlineonline]. Available: https://fr.wikipedia.org/wiki/Sel_de_Seignette#:~:text=Le%20sel%20de%20Seignette%20ou,antioxydant%20et%20r%C3%A9gulateur%20de%20pH..

[14] D. Samah, "Electromechanical impedance analysis of the behavior of ultrasonic piezoelectric transducers in cavitating media," Toulouse, 2012.

[15] Y. Zhao, "Capacitive micromachined ultrasonic transducers for transmitting and receiving ultrasound in air," 2019.

[16] SCHWEITZER S.A.S , "FICHE TECHNIQUE PAPIER ALUMINIUM," [En online]. Available: https://www.lamaison.fr/media/pdf/product/111879/technical_datasheet_pdf//54ec676724b1d65138e86449d2d1f6e25018d876_EMB200AL03894_001.pdf.

# APPENDICES

## Appendix 1: Project statement

**PROJET de FIN D'ETUDES**

**TITRE DU PROJET :**

**Conception, Fabrication et Caractérisation de microsystèmes électromagnétiques et piézoélectriques dit *lowtech***

**DESCRIPTION :**

De nos jours les approches *lowtech* se développent afin de ménager les ressources environnementales limitées de notre planète. Celles-ci sont particulièrement adaptées aux dispositifs dédiés à la formation ou la pédagogie. Récemment, des microsystèmes électromagnétiques ont pu être fabriqués avec des moyens de prototypage limités de type *fablab*. De plus, des structures à base de sels piézoélectriques ont déjà montrés des preuves de faisabilités [2] et peuvent être miniaturisés afin de proposer des microsystèmes piézoélectriques inédits et *lowtech*.
Ce projet vise donc à concevoir, fabriquer puis caractériser des microsystèmes électromagnétiques et piézoélectriques *lowtech* sur la base des techniques et procédés déjà montrés, comme point de départ. Ces structures pourront être ensuite utilisées, ou répliquées dans un cadre pédagogique pour le module microsystèmes de 5ieme année dans le futur.

[1] : Lemaire, E., Thuau, D., Caillard, B., & Dufour, I. (2015). Fast-fabrication process for low environmental impact microsystems. *Journal of cleaner production, 108*, 207-216.
[2] : Lemaire, E., Moser, R., Borsa, C. J., & Briand, D. (2016). Green paper-based piezoelectronics for sensors and actuators. Sensors and Actuators A: Physical, 244, 285-291.

**OBJECTIFS**

Déroulé proposé :

- Etude bibliographique & recherche
- Design
- Fabrication
- Caractérisation & Traitement & Modélisation
- Valorisation & documentation du projet

| | |
|---|---|
| ORGANISME(S) CONCERNE(S) | DEE – GREMAN |
| NOMBRE D'ETUDIANTS | 1 ou 2 |
| RESPONSABLE(S) ENSEIGNANT (S) | M. Lemaire |
| LIEU | DEE |

## Appendix 2: Project poster

GREMAN

université de TOURS | POLYTECH TOURS

# Conception, Fabrication et Caractérisation de microsystèmes *low-Tech*

Projet de fin d'études

*JABRI Ismail encadré par LEMAIRE Etienne*

## Introduction

- Les microsystèmes électromécaniques (MEMS) sont des dispositifs miniaturisés intégrant des éléments mobiles/vibrants pour réaliser des applications allant des capteurs d'accélération jusqu'à l'imagerie médicale...
- Dans un contexte de développement durable, ce projet vise à concevoir, fabriquer et caractériser deux types de microsystèmes à faible technologie (lowtech):
  - Les CMUT (Capacitive Micromachined Ultrasonic Transducers), exploitant des membranes pour générer des ondes ultrasonores.
  - Les cantilevers, des MEMS de type poutre en porte-à-faux.

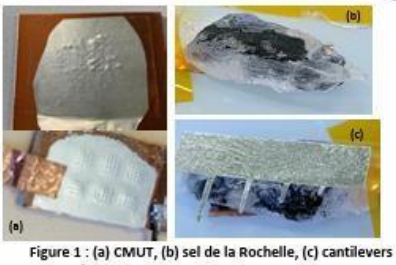


**Figure 1 : (a) CMUT, (b) sel de la Rochelle, (c) cantilevers actionnés par le sel de la Rochelle.**

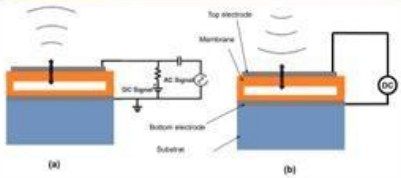


**Figure 2 : Principe du CMUT (a) en transmission alimenté en DC superposée à une tension AC pour générer une onde ultrasonore et (b) en réception alimenté qu'avec la tension DC pour le polariser**

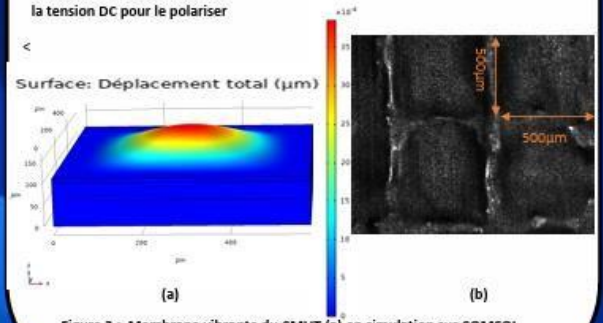


**Figure 3 : Membrane vibrante du CMUT (a) en simulation sur COMSOL Multiphysics et (b) dimension d'une cavité mesurée au vibromètre laser**

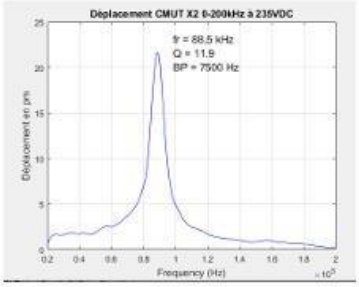


**Figure 4 : Déplacement (pm) en fonction de la fréquence 0-200 kHz, mesuré au vibromètre laser à Vdc = 235 V et VChirp = 10 Vpp.**

- Le facteur de qualité Q = 11.9 traduit la capacité du CMUT à fonctionner efficacement dans une plage de fréquences spécifique qui est dans ce cas de +/-3500 Hz centrée autour de la fréquence centrale de 88.5kHz.

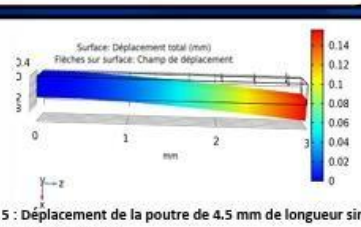


**Figure 5 : Déplacement de la poutre de 4.5 mm de longueur simulé sur COMSOL Multiphysics**

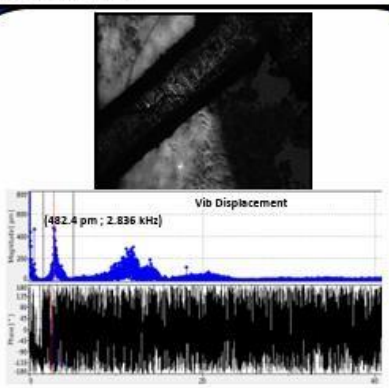


**Figure 6 : Déplacement (pm) de la poutre en fonction de la fréquence 0-40 kHz, mesuré au vibromètre laser à Vdc = 2V, et VChirp = 10 Vpp**

- La poutre a un mode propre principal à 2836 Hz. Les autres modes observés sont ceux du cristal piézoélectrique de sel de Rochelle. Ces modes sont utiles dans des applications de détection des vibrations, de gaz...

## Conclusion

- Les transducteurs CMUT et cantilevers low-Tech dont la réponse en fréquence a été démontrée, n'ont pas vocation à être intégrables directement dans des applications industrielles. Cependant, ils sont de bon candidat pour une utilisation pédagogique afin d'expérimenter une technologie similaire à celle mis en œuvre sur silicium avec un haut niveau de performance.
- La miniaturisation des CMUTs se traduit par une fréquence de résonance plus élevée, améliorant la résolution spatiale dans l'imagerie médicale. Quant aux cantilevers, la précision de la détection augmente lorsque le comportement vibratoire (modes propres) est bien défini.

## Appendix 3: Forecast and actual Gantt charts

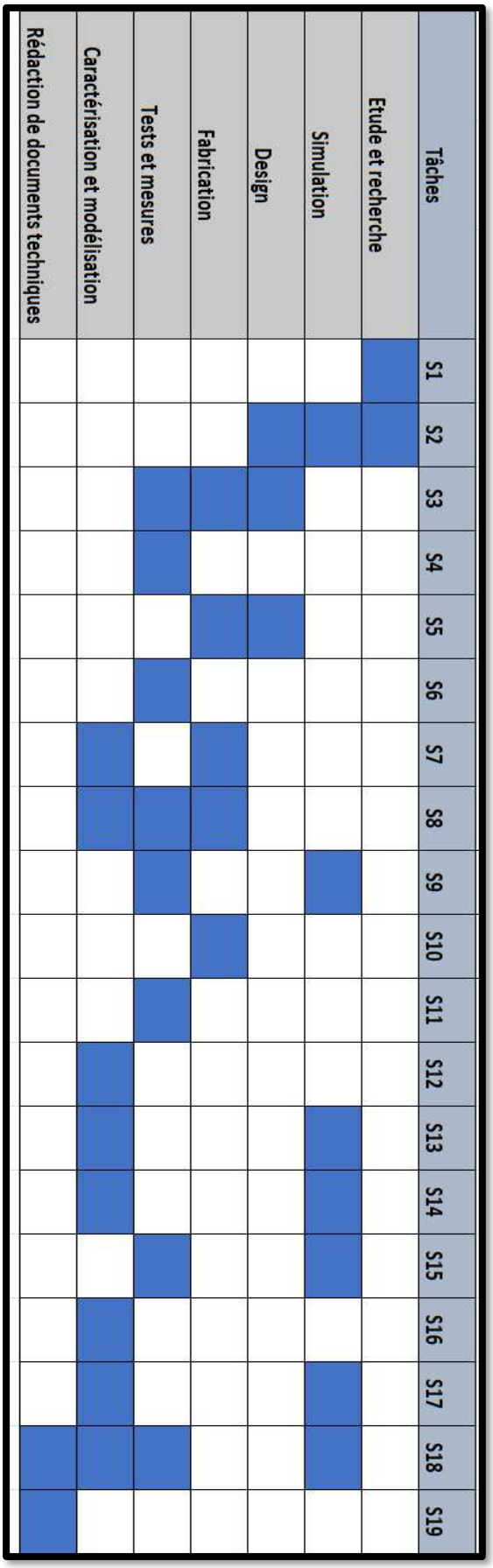


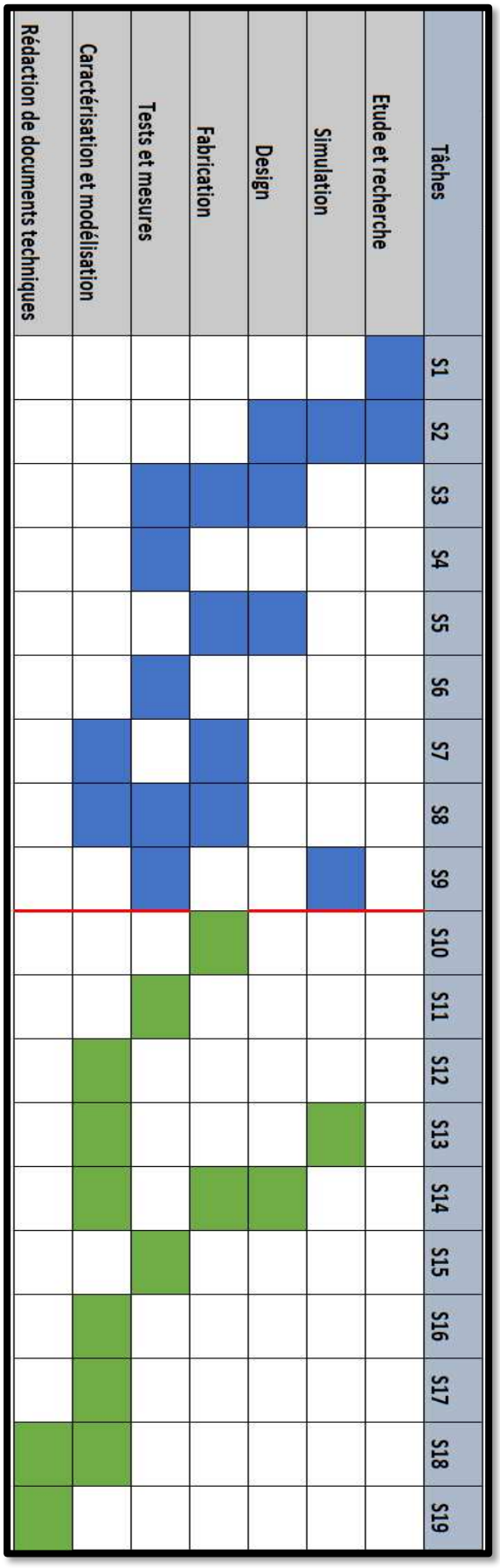

## Appendix 4: The smallest laser-cut cavities

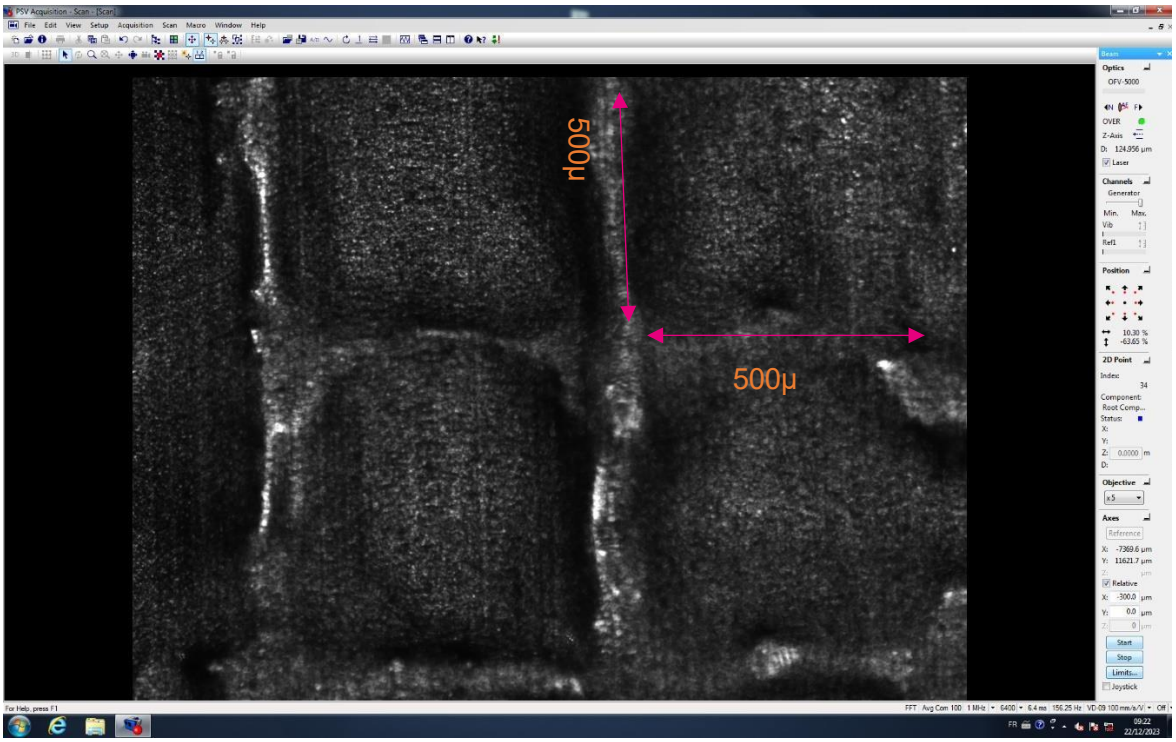


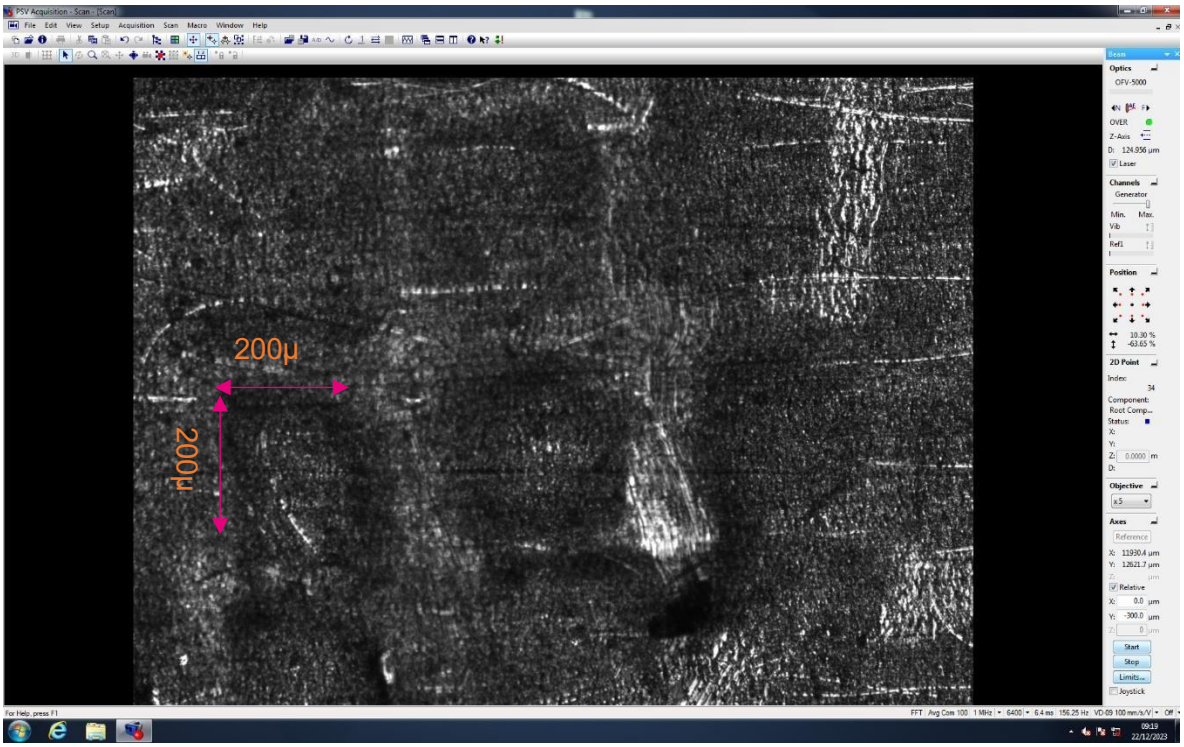

Appendix 5: First eigenmode of a 4.5 mm long beam actuated by a piezoelectric pad

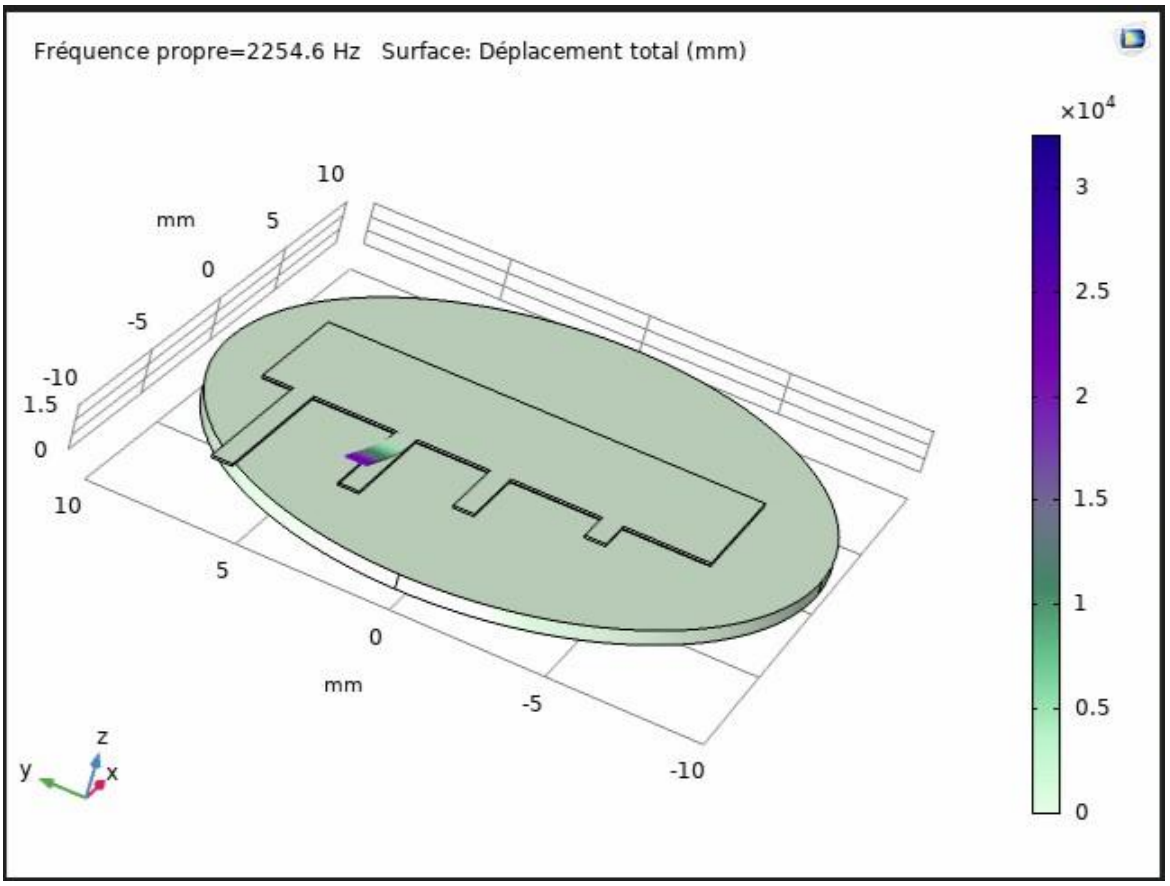


Appendix 6: CMUT simulation with small cavities.

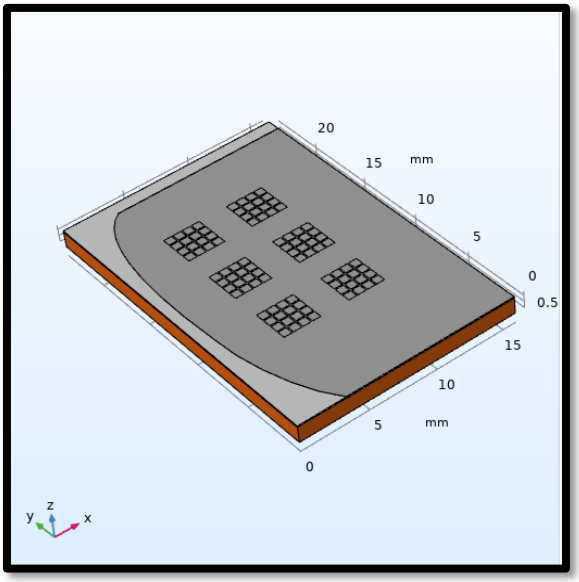


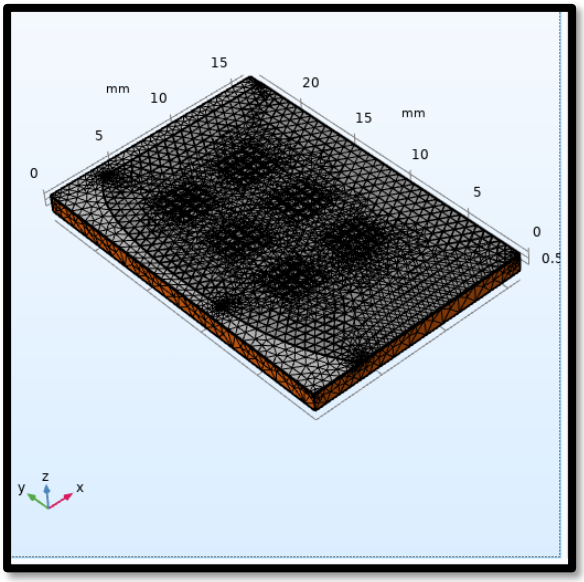

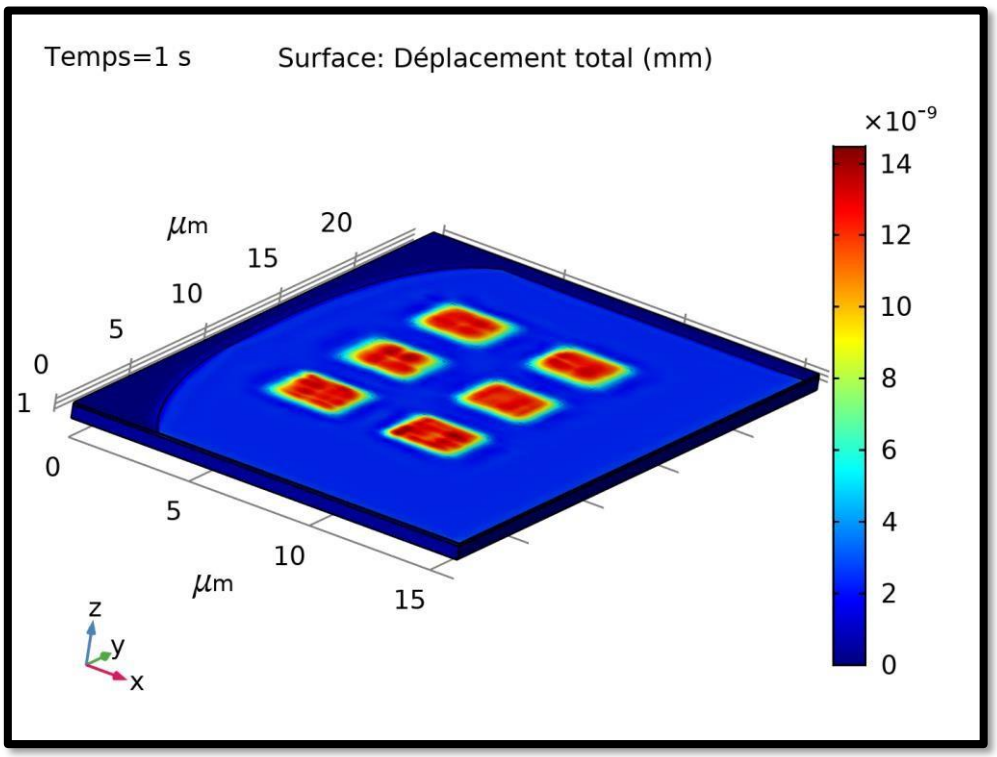
Temps=1 s
Surface: Déplacement total (mm)
×10⁻⁹
14
12
10
8
6
4
2
0
μm
20
15
10
5
0
1
0
5
10
15
μm
z
y
x

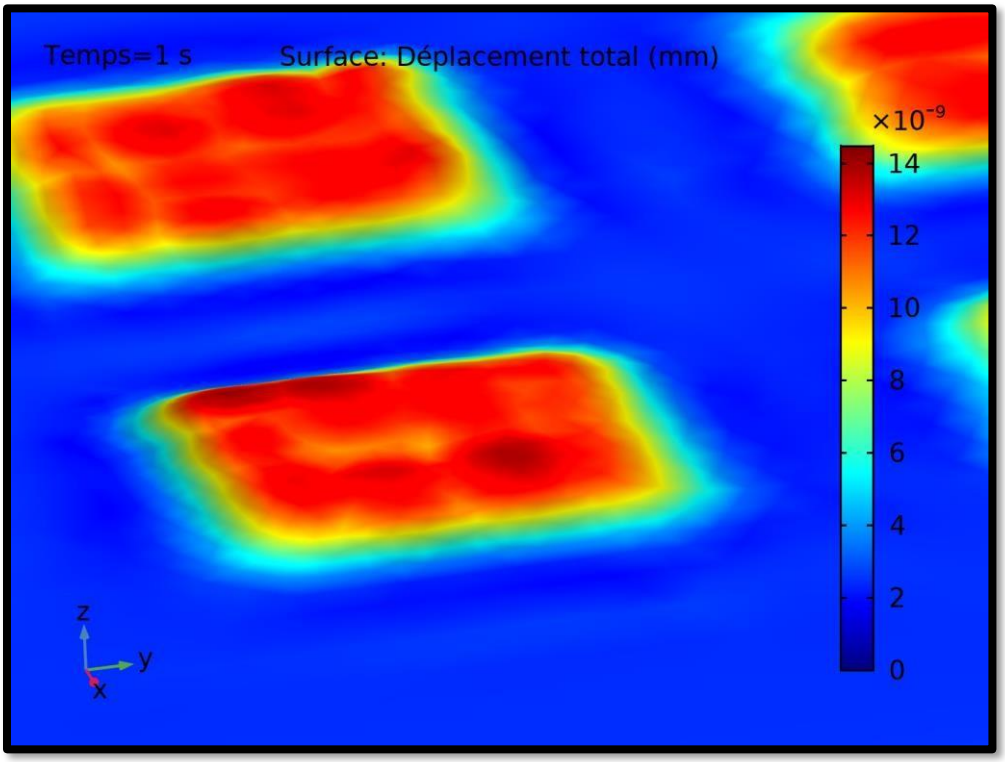
Temps=1 s
Surface: Déplacement total (mm)
×10⁻⁹
14
12
10
8
6
4
2
0
z
y
x

Appendix 7: Vibration velocity in µm/s as a function of frequency 0-100 kHz measured with a laser vibrometer

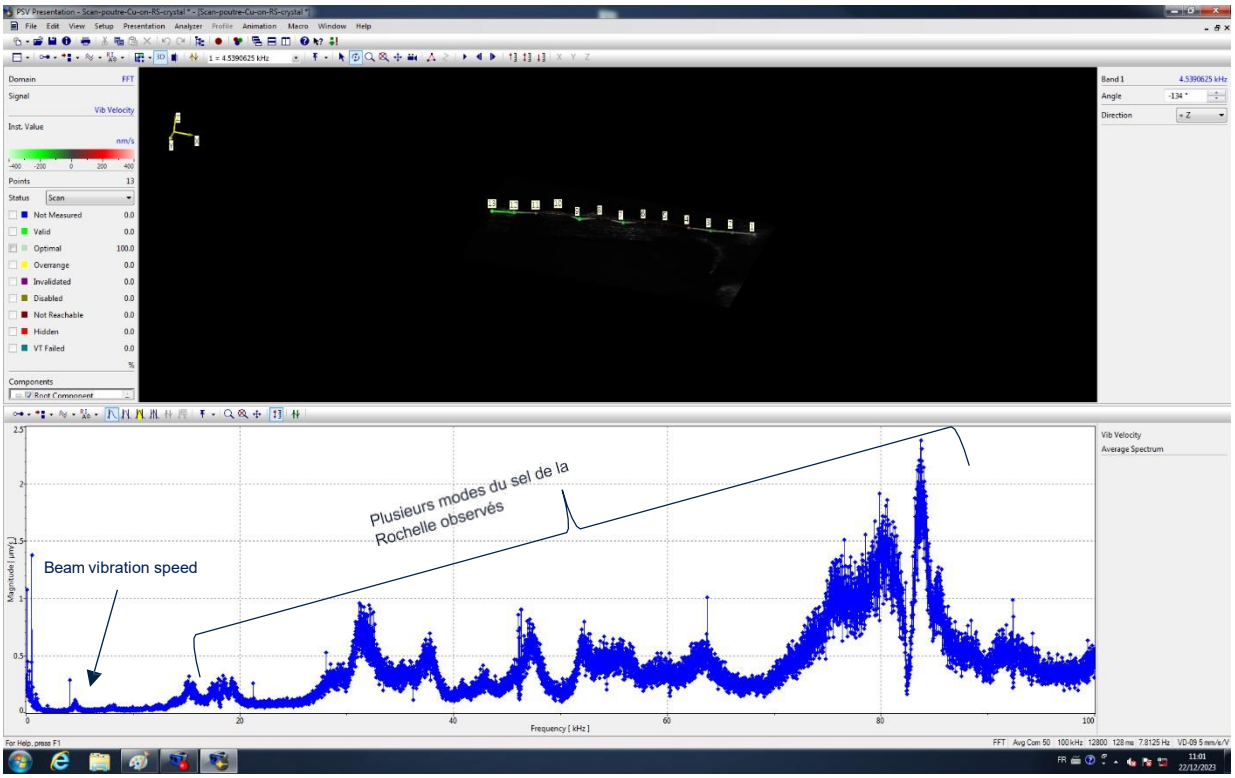

Ismail JABRI

# Design, manufacture and characterization of low-tech microsystems

Summary:

This project focuses on the design, manufacture and characterization of low-tech microsystems (MEMS) for educational applications. The three main types of microsystems include the CMUT (Capacitive Micromachined Ultrasonic Transducer), cantilevers and the U-wire electromagnetic transducer. Affordable and environmentally-friendly materials used include copper, aluminum, metallized PET, polypropylene and Rochelle salt. Finite element simulations were used to understand the physical behavior of the transducers, focusing on membrane displacements, mechanical stresses and natural frequencies. Using experimental characterization, the performance and limitations of these microsystems were assessed. For CMUTs, miniaturization leads to a higher resonance frequency, improving the resolution of non-destructive detection. Cantilevers can be operated around their natural frequencies. U-wires are versatile and efficient, given their high electromagnetic torque.

*Keywords: MEMS, CMUT, sel de la Rochelle, cantilevers, transducers, low-Tech*

Résumé :

Ce projet centré sur la conception, la fabrication, et la caractérisation de microsystèmes (MEMS) à faible technologie pour des applications pédagogiques. Les trois principaux types de microsystèmes inclus le CMUT (Transducteur Ultrasonique Micro-usiné Capacitif), les cantilevers et le transducteur électromagnétique en forme de fil en U. Des matériaux abordables et écologiques utilisés ont été utilisés comprennent le cuivre, l'aluminium, le PET métallisé, le polypropylène et le sel de la Rochelle. Les simulations par éléments finis ont permis de comprendre le comportement physique des transducteurs, mettant l'accent sur les déplacements des membranes, les contraintes mécaniques et les fréquences propres. À l'aide de la caractérisation expérimentale, les performances et les limites de ces microsystèmes ont été évaluées. Pour les CMUT, une miniaturisation conduit à une fréquence de résonance plus grande, améliorant la résolution de la détection non destructive. Les cantilevers peuvent être exploités autour de leurs fréquences propres. Le fil en U est polyvalent et efficace tant le couple électromagnétique est fort.

*Mots clés : MEMS, CMUT, sel de la Rochelle, cantilevers, transducteurs, low-Tech*